Research Article Open Access

Sphumelele C. Ndlovu and Naven Chetty*

Experimental determination of thermal turbulence effects on a propagating laser beam

DOI 10.1515/phys-2015-0028

Received September 08, 2014; accepted February 03, 2015

Abstract: The effect of turbulence on propagating laser beams has been a subject of interest since the evolution of lasers back in 1959. In this work, an inexpensive and reliable technique for producing interferograms using a point diffraction interferometer (PDI) was considered to experimentally study the turbulence effects on a laser beam propagating through air. The formed interferograms from a propagating beam were observed and digitally processed to study the strength of atmospheric turbulence. This technique was found to be sensitive enough to detect changes in applied temperature with distance between the simulated turbulence and laser path. These preliminary findings indicated that we can use a PDI method to detect and localise atmospheric turbulence parameters. Such parameters are very important for use in the military (defence laser weapons) and this is vital for South Africa (SA) since it has natural resources, is involved in peace keeping and mediation for other countries, and hence must have a strong defence system that will be able to locate, detect and destroy incoming missiles and other threatening atmospheric systems in order to protect its environment and avoid the initiation of countermeasures on its land.

Keywords: thermal turbulence; point diffraction interferometry; intensity perturbations

PACS: 06.60.-c; 07.60.-j; 42.60.-v; 42.62.-b

1 Introduction

The study of the behavior of a laser beam propagating in the atmosphere plays a crucial role in defence laser weapons [1, 2]. Many theoretical and experimental investigations on the behavior of a propagating beam show

Sphumelele C. Ndlovu: School of Chemistry and Physics, University of KwaZulu-Natal, Scottsville, Pietermaritzburg 3209, RSA *Corresponding Author: Naven Chetty: School of Chemistry and Physics, University of KwaZulu-Natal, Scottsville, Pietermaritzburg 3209, RSA, E-mail: ChettyN3@ukzn.ac.za

that atmospheric turbulence leads to intensity perturbations [3-9]. These perturbations result from refractive index fluctuations due to thermal fluctuations in the atmosphere. Published work shows that measurements of the intensity fluctuations have been of great interest for many vears, and different methods have been developed [10–17]to classify the impact of such turbulence on a propagating laser beam. Some of these methods are very similar, such as the Twyman-Green interferometer used by Twyman [18] and the Fizeau interferometer used by Burge [19] which produces fringes of equal thickness. Other methods of measuring thermal effects on a propagating laser beam require bulky or expensive specialized equipment. Such experiments are not easy to construct in the laboratory and involve complicated mathematical manipulation and/or modelling [20-24]. In this work, a point diffraction interferometer (PDI), also known as Smartt interferometer, was used to obtain interferograms from a laser beam propagating through air in the laboratory.

The concept of PDI was first described by Linnik [25], and was later developed by Smartt [26, 27]. A PDI is a common-path interferometer which is simple to construct, easy to align measures the optical wavefront and subsequently produces interferograms from the use of a single laser beam through a PDI pinhole. These interferograms can be used to extract valuable wavefront information such as turbulence strength, and inner and outer scales of turbulence. The PDI used in this work consisted of a metal plate with different sizes of pinholes punched into its surface. Light incident on the PDI plate can be diffracted by the PDI pinhole thus allowing some of the light to pass through to form a spherical wavefront on the other side of the PDI plate. Strategically placing collimating lenses along the optical train can minimize beam spreading and thus contribute to interferograms that are free from edge effects and are also of good contrast. In this experiment, clear and bright interferograms were very important as they provided maximum visibility of intensity perturbations resulting from the introduced thermal turbulence. It has been experimentally shown that a laser beam propagating through turbulence suffers wandering [28], spreading [29], scintillation [30] and many other behaviors. Beam wandering is defined as the change of direction of the propagating beam that results from the introduction of turbulence. This subject is of interest to those researchers working on laser optics, and those working on defence laser weapons to ensure accuracy.

A Gaussian beam can be obtained by shaping, focusing and modifying the laser beam using collimating lenses. However, at any point a laser beam can still acquire curvature and begin spreading in accordance with,

$$R(z) = z \left[1 + \left(\frac{\pi w_0^2}{\lambda z} \right)^2 \right], \tag{1}$$

and

$$w(z) = w_0 \left[1 + \left(\frac{\lambda z}{\pi w_0^2} \right)^2 \right]^{\frac{1}{2}},$$
 (2)

where z is the distance propagated from the plane where the wavefront is flat, λ is the wavelength of the laser beam, w_0 is the radius of the $1/e^2$ irradiance contour at the plane where the wavefront is flat, w(z) is the radius of the $1/e^2$ contour after the waves have propagated a distance z, and R(z) is the wavefront radius of curvature after propagating a distance, z. The irradiance distribution of the beam depends mainly on the total power, illustrated as,

$$I(r) = I_0 e^{-2r^2/w^2}, (3)$$

where w=w(z), r is the radial distance from the centre axis of the beam, $I_0=\frac{2P}{\pi w^2}$, is the amplitude of the irradiance distribution and P is the total power in the beam which is the same at all cross sections of the beam. The propagation distance in this work is short, less than 2 m, thus the total power of the beam is assumed to be constant.

A cigarette lighter can be used to introduce weak turbulence to the environment. Analysis of the effects of thermal turbulence on a laser beam propagating through weak turbulence is achieved by using the Rytov method [31, 32]. It is necessary, when using the Rytov method, to define the field of the wave as

$$E(r) = e^{\phi(r)},\tag{4}$$

which leads to a series solution for *E* defined as [31, 32],

$$E(r) = e^{(\phi_0 + \phi_1 + \phi_2 + \dots)}.$$
 (5)

In the above expression ϕ_1 is the first approximation of the effect of the random medium through which the wave passes. The first approximation, ϕ_1 , normally takes the form [31, 32],

$$\phi_1(r) = \chi + jS_1, \tag{6}$$

where ϕ_1 represents the first order fluctuation of the amplitude of the wave [31, 32] and S_1 is the first-order phase

fluctuations. Rytov's solution for the intensity variance under weak turbulence is approximated by the log intensity as [31, 32],

$$\sigma_I^2 = 1.23 C_n^2 k^{7/6} L^{11/6}, \tag{7}$$

where C_n^2 is the refractive index structure constant, k is the wave number and L is the optical path length. This notation indicates that the variance holds in the Rytov region of weak turbulence [31, 32]. The variance of the log intensity fluctuations in Equation 7 increases, without limits, as the strength of turbulence and range of path length increases. Traditionally, the variance of the intensity fluctuations is saturated when there is an increase in turbulence which increases the irradiance fluctuations, and hence the strength of turbulence increases. In this work, the observed intensity variance under conditions of weak turbulence is approximated by the log intensity as described in [31, 32]. This was also recently verified by [33], where an analysis on the fluctuations of a laser beam due to weak thermal turbulence effects illustrated a Rytov weak fluctuation parameter less than 0.3.

2 Experiment

The schematic diagram (Figure 1) is the complete optical train set-up with labels L = light source assembly, N = neutral density filter, M = calibration module, C = collimating lenses, S = spatial filter and the PDI is mounted on a carrier cell.

The optical bench

The entire laboratory experiment was set-up on a 1.2 m by 1.8 m granite optical table. This table isolates the optical components in the receiver train from vibrations that may be caused by the surroundings. The granite table has a flat homogeneous surface which made it easy to align the main receiver train with the light source.

The dovetail rail

A 91.44 cm Edmund "dovetail" v-block rail was used for the main receiver train. The rail was divided into 3 sec-



Figure 1: The complete layout of the optical train is represented by grey blocks. Thermal turbulence was induced in the 200 mm gap between the neutral density filter (N) and the point marked A on the calibration module.



Figure 2: The complete receiver optical train with the PDI plate shown in yellow, located right in-front of the camera on the XYZ stage and carrier cell. The complete PDI assembly is shown in Figure 3.



Figure 3: An Edmund XYZ stage and carrier cell with PDI (in front of the camera) is illustrated in this figure.

tions. A 60.96 cm rail was used to hold the collimating lenses and two 15.24 cm sections, one each for the light source assembly and camera assembly. All the rails were supported by and screwed down onto 150 mm by 150 mm Edmund 53936 bench plates of 13 mm thickness. There were 5 bench plates that were used to mount the dovetail rails. Each bench plate was furnished with M6 holes arrayed on a pitch of 25 mm. This helped in aligning optical components with the light source.

The light source

A JD-950 20 mW green laser of wavelength 532 nm was mounted together with a microscope objective and collimating lens of 160 mm focal length. The collimating lens produced a coherent beam of light of diameter 25 mm. The microscope objective reduced the beam by 20 times 0.35 (numerical aperture) to a point where it was collimated by the collimating lens on the right of the microoptical bench. The light source assembly consisted of a laser diode, a plastic aspheric collimator and holographic diffuser. The plastic collimator and the holographic diffuser were mounted in separate 25 mm T-mount cells. The light source assembly was mounted on a micro-optical bench which was glued onto a 61 dovetail rail to avoid movements and vibrations from the surroundings.

A reflective 50 mm by 50 mm 3.0 OD neutral density filter of 1.5 mm thickness manufactured by Edmund optics

was placed just in front of the light source. This reflective filter helped in reducing the laser beam intensity and eliminates stray-light artefacts so that clear and bright interferograms were produced for analysis. The simulated turbulence was introduced in the 200 mm gap between the light source assembly and the main receiver train.

The collimators

Three identical collimating lenses, each 121.5 mm long of 200 mm focal length, were placed on a 60.96 cm dovetail rail. The lenses were moved forwards and backwards along the train to focus, shape and modify the Gaussian beam by noting the size of the beam formed on the PDI plate. A smaller sized beam was necessary to allow the beam to pass through the PDI pinhole. The collimators were also used to minimize beam wandering and spreading.

The PDI

A point diffraction interferometer (PDI) manufactured by Astro Electronics was used in this work. It consisted of 55 pinholes which were distributed on an array of pitch 1mm. The PDI was mounted together with the carrier cell on an Edmund XYZ stage. There were three adjustments on the XYZ stage that were used to locate the laser beam so that it would pass through the PDI pinhole. The PDI was mounted between the collimators and the camera assembly so that the beam would pass through the pinhole and interferograms would be formed. This type of interferometry was used since it is simple to align and it uses a single laser beam to produce clear and bright interferograms. The PDI was positioned at a distance of 872.10 mm with reference to the module at point A in Figure 1. This helped in locating the beam after it had been collimated by the lenses.

The camera

A Nikon D3100 camera was mounted on a 15.24 cm dovetail rail. This was held in place by a strap-down bar, in order to hold and lock the camera onto the bench plate to prevent movements and reduce distortions of the interferograms caused by the surroundings. The camera consisted of a doublet lens of 150 mm in focal length. This lens helped in focusing the formed fringes from the PDI pinhole for good visualisation on the screen (monitor). The camera was used to take colour videos and still images. The camera had an output of High Definition Multimedia Interface (HDMI). Pictures obtained from the camera were saved onto a 4 gigabyte micro SD memory card. The obtained pictures of interferograms were then transferred to a computer. Computer software discussed in section 2.8 was used to analyse these pictures.

The monitor

A 24-inch Samsung monitor screen with an HDMI input helped to display the live video. This monitor was con-

nected to the camera through an HDMI cable with C-style mini-HDMI male connector. The monitor was used to display the images and videos taken by the camera.

Interferograms analysis

Preliminary results were obtained using ImageJ computer software. The data obtained from this software was then compared to results predicted by theory and found by other workers.

Experimental procedure

To test the effectiveness of the above experimental setup, a cigarette lighter was used as the source of the applied turbulence. It was introduced in the "turbulence gap" but was not directed towards the propagating laser beam. This source of thermal turbulence was chosen for the fact that it applies stable thermal turbulence which increases in close proximity to the propagating beam. The change in temperature within the turbulent region was measured using a j-type thermocouple.

The source of turbulence was switched on for a few minutes to enable fully developed thermal turbulence to ensue. The laser beam then passed through this turbulent region before reaching the collimators and the PDI. Random fluctuations in the laser beam direction resulted directly from refractive index variations due to temperature variations created by the thermal turbulence of the cigarette lighter. These turbulations affect the propagation of the laser beam by changing its structure, and this can be visualized from the produced interferograms. It was considered that if the proposed method is able to effectively produce clear interferograms which exhibit interference patterns, the experimental setup and technique may then be used for a more detailed analysis.

3 Results and discussion

More experimental work needs to be done to verify and reduce the existing experimental difficulties with laser beam propagation [34, 35]. An experiment to measure intensity perturbations of a laser beam propagating through air was developed and conducted in a dark room which had been painted black to minimize the contamination of the produced interferograms from stray/environmental room light. Room temperature fluctuations due to environmental conditions were minimal (0.50°C over an experimental period). The change in the room temperature closest to the propagating beam was influenced by the amount of heat produced by the cigarette lighter. An interferogram (Figure 4) of an unperturbed beam in the absence of any there

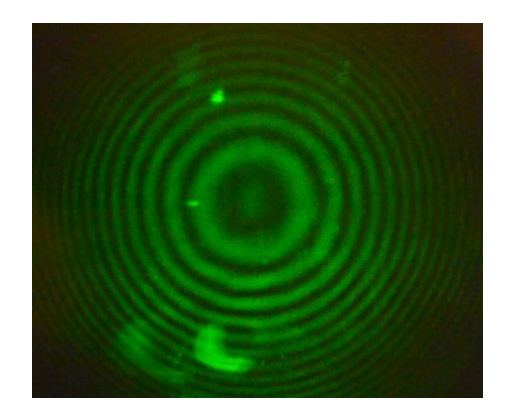


Figure 4: Interferogram with some stray-light artefacts on an unperturbed beam. Image size: Width = 448 pixels, Height = 372 pixels.

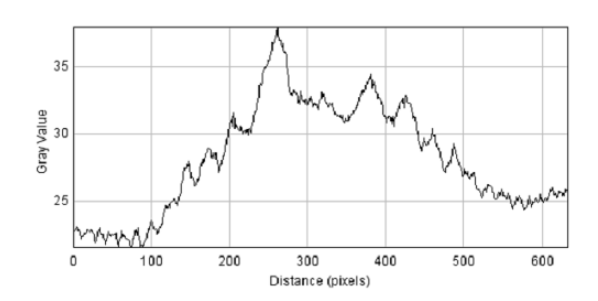


Figure 5: A representation of the interferogram profile plot with stray light artefacts on an unperturbed beam.

mal turbulence and with proper optical alignment, shows some stray light artefacts.

Numerous artefacts were observed in the interference pattern and this is indicative of stray light. The presence of stray light artefacts can compromise the experimental results and prevent the true effect of the thermal turbulence from being analysed and quantified. Such stray light can over or under-compensate for the thermal turbulence effect. This type of light resulted from the reflection of the laser light off the optical components and back onto the detector. A stray light correction was necessary. This was achieved by placing a neutral density filter in front of the light source and tilting it by a small angle (about 2 degrees). Thus, no light from the receiver train was reflected back onto the light source assembly or the objective lens. The importance of removing stray light when performing the experiment was to ensure that the observed interferograms were bright and clear so that the plot profile in Figure 5 was avoided in the experiment.

The plot profile in Figure 5 illustrates a cross-section of the light intensity profile as a gray value which indicates that the stray light is of a very strong intensity and thus overshadows the actual intensity of the interference pattern, making analysis of the interference pattern impossi-

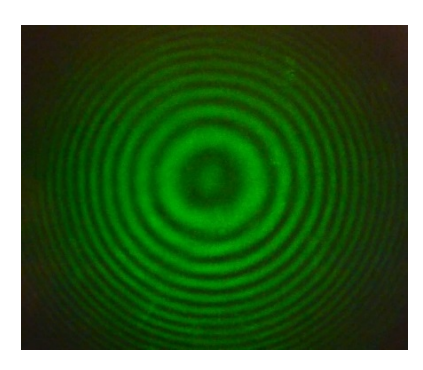


Figure 6: Interferogram of an unperturbed laser beam propagating through air. Image size: Width = 436 pixels, Height = 366 pixels.

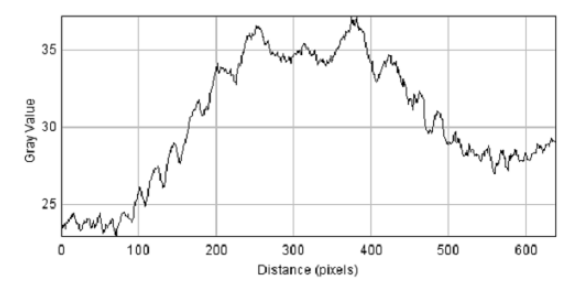


Figure 7: Profile plot from an unperturbed laser beam with a higher gray value on the right due to imperfections in the lenses.

ble since it is buried in the noise of the stray light. If there are no stray-lights, Figure 5 should be symmetrical about the gray value and be similar to Figure 6.

The intensity distribution of interferograms (Figure 7) produced from an unperturbed beam before commencing with thermal agitation. This was used as reference when analysing the perturbed interferograms.

The intensity distribution of a perturbed beam changed dramatically when compared with that of an unperturbed beam. Figure 8 indicated that the increase in temperature near a propagating beam distorts the beam's

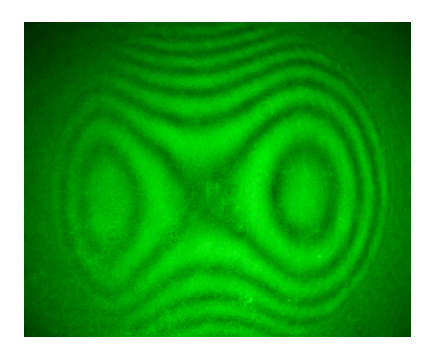


Figure 8: Interferograms obtained from a beam perturbed with a cigarette lighter. Image size: Width = 428 pixels, Height = 348 pixels.

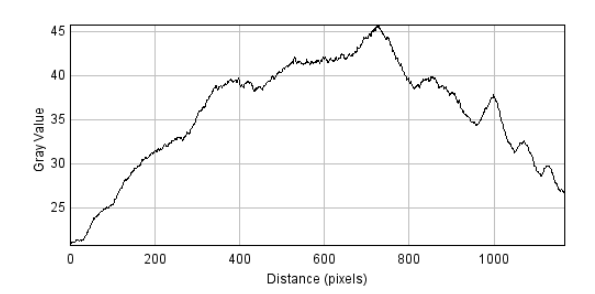


Figure 9: Profile plot obtained from a perturbed beam propagating through a heated region.

Table 1: The average change in temperature with distance from laser light source to point A.

Distance (mm)	Temperature (°C)
0	25.5
60	39.1
120	56.5
140	49.4
160	39.5
200	27.1

wavefront and its intensity distribution is shown in Figure 9.

A cigarette lighter placed 120 mm from the light source and 50 mm below the propagating beam showed an average temperature of 56.5° C as measured by a thermocouple 100 mm away from the light source. This temperature distance dependence (see Table 1) also has an effect on the interferograms formed.

The Rytov's approximation of weak turbulence indicates that the increase in thermal turbulence can cause intensity fluctuations. This is illustrated by an increase in intensity of the perturbed beams when compared to unperturbed beams. It is also apparent that energy redistribution occurs on the propagation beam. This is indicated by the intensity distribution of the perturbed beam in Figure 9, with a maximum peak in gray value between 400 and 800 pixels, whereas in Figure 7 the peak follows a narrow Gaussian distribution between 250 and 370 pixels.

4 Conclusion

In conclusion, we have effectively developed and tested an inexpensive, but very robust laboratory experiment to detect thermal turbulence effects on a laser beam propagating through a PDI pinhole. Preliminary results showed that the propagating laser beam is dramatically affected by a

change $(\pm 25^{\circ}\text{C})$ in temperature arising from applied turbulence. The temperature fluctuations result in changes in the refractive index of air, and thus changes in the beam propagation profile.

Future work will consider these preliminary results and analyse them using a more appropriate and comprehensive technique, such as Fast Fourier Transform. This information can then be used to fully classify the exact effect of thermal turbulence on laser beam propagation. Also of interest to us is the nature and extent to which other lasers are affected by directional turbulence, and particularly the Kolmogorov theory [36]. This may then be used as a comparative study for future field work. Such results are sought by many research groups, especially those working with lasers and laser optics.

The beam displayed propagation patterns which included the redistribution of energy, scintillation, wandering and spreading and this has also been proved in [33, 37]. However difficulties are not only encountered in experimental studies; recent work has shown this to be numerically challenging as well [38, 39]. The experimentally obtained results will need to be comprehensively classified to be of use to the optical research community. Different light sources, together with varying thermal and directional turbulence sources, will be used in future work to verify these initial results.

Using a 1550 nm or 1064 nm laser, instead of a visible laser (532 nm), means that the wavelength is increased. An increase in wavelength can decrease the wavenumber k, which is directly proportional to intensity variance as indicated by Equation 7. Hence an increase in wavelength decreases the intensity variance. This was not visible enough for our camera and we were not able to observe the fringes, thus a more sensitive light detector will be required in order to observe the behavior of such a beam as it propagates through a PDI pinhole for future work.

Acknowledgement: The authors wish to thank Mr. Derek Griffith for his immense contribution to the experimental design and set-up as well as for the numerous discussions and helpful comments. The Council for Science and Industrial Research (CSIR) and ARMSCOR are thanked for the generous support for the student as well as for the laboratory equipment.

References

 D.H. Titterton, A review of optical countermeasures, in Conference on Technologies for Optical Countermeasures, October 25,

- 2004, London, UK (London, 2004)
- [2] D.H. Titterton, The development of infrared countermeasure technology and systems, In A. Krier (Ed.) (Springer-Verlang, London, 2005)
- [3] H. Weichel, Laser beam propagation in the atmosphere (SPIE, Berlin, 1990)
- [4] R.J. Cook, J. Opt. Soc. Am. A 65, 942 (1975)
- [5] E. Golbraik, H. Branover, A. Zilberman, Nonlinear Proc. Geoph. 13, 297 (2006)
- [6] R.L. Fante, Proc. IEEE 63, 1669 (1975)
- [7] L.G. Wang, W.W. Zheng, J. Opt. A: Pure Appl. Opt. 11, 065703 (2009)
- [8] E.N. Nyobe, E. Pemha, PIER 53, 31 (2005)
- [9] T. Shirai, J. Opt. Soc. Am. A 20, 1094 (2003)
- [10] L.A. Chernov, Wave propagation in a random medium (McGraw-Hill, New York, 1960)
- [11] V.I. Tatarskii, Wave propagation in a turbulent medium (McGraw-Hill, New York, 1961)
- [12] V.I. Klyatskin, V.I. Tatarskii, Radiofizika 15, 1433 (1972)
- [13] L.C. Andrews, M.A. Al-Habash, Wave. Random Media 11, 271 (2001)
- [14] A. Consortini, Y.Y. Sun, G. Conforti, J. Mod. Opt. 37, 1555 (1990)
- [15] A. Consortini, G. Fusco, Y.Y. Sun, Wave. Random Media 7, 521 (1997)
- [16] C. Fan, Chinese J. Quantum Electro. 16, 519 (1999)
- [17] J. Hona, E. Pemha, PIER 84, 289 (2008)
- [18] F. Twyman, Astro. J. 48, 256 (1918)
- [19] J. Burge, SPIE 2536, 127 (1995)
- [20] A. Zilberman, N.S. Kopeika, P Soc. Photo-Opt. Ins. 5891, 129 (2004)
- [21] A. Zilberman, N. Kopeika, J. Appl. Remote Sens. 2, 023540 (2008)
- [22] B.A. Bachmann, S. Hammel, SPIE Proceedings 8161, 816109 (2011)
- [23] D. Coburn, D. Garnier, J. Dainty, SPIE Proceedings 598, 105 (2005)
- [24] T. Butterley, R.W. Wilson, J.L. Aviles, Proceedings of the Optical Turbulence Characterization for Astronomical Applications, 58 (2008)
- [25] M.M. Miroshnikov, J. Opt. Tech. 77, 401 (2010)
- [26] R.N. Smartt, J. Strong, J. Opt. Soc. Am. 62, 737 (1972)
- [27] R.N. Smartt, W.H. Steel, Jpn. J. Appl. Phys. 14, 351 (1975)
- [28] H. Kaushal, IEEE Photon. Technol. Lett. 23, 1691 (2011)
- [29] T. Wang, Z. Chen, Opt. Comm. 282, 1255 (2009)
- [30] L. Xianhe, P. Jixiong, Opt. Express 19, 26444 (2011)
- [31] H. Yuskel, Studies of the effects of atmospheric turbulence on free space optical communications, PHD Thesis (University of Maryland, 2005)
- [32] L.C. Andrews, R.L. Phillips, Laser beam propagation through random media (SPIE Press, Bellingham, 1998)
- [33] S.C. Ndlovu, N. Chetty, Cent. Eur. J. Phys. 12, 466 (2014)
- [34] R.S. Lawrence, J.W. Strohbehn, Proc. IEEE 58, 1523 (1970)
- [35] J.R. Kerr, J.R. Dunphy, JOSA 63, 1 (1973)
- [36] U. Frisch, Turbulence (Cambridge University Press, Cambridge, 1995)
- [37] A. Chaibi, C. Mafusire, A. Forbes, J. Opt. 15, 105706 (2013)
- [38] M. Carnevale, F. Montomoli, A. D'Ammaro, S. Salvadori, F. Martelli, ASME J. Turbomach. 135, 051021 (2013)
- [39] C. Bernardini, M. Carnevale, S. Salvadori, F. Martelli, WSEAS T. Fluid Mech. 6, 160 (2011)